

Short Communication

A potential Green Anti-scaling and Corrosion Inhibitor for Mild Steel in Brine Solution

R.H. Khaled¹, A.M. Abdel-Gaber^{2,*}, H.T. Rahal¹, R. Awad³

¹ Department of Chemistry, Faculty of Science, Beirut Arab University, Lebanon

² Department of Chemistry, Faculty of Science Alexandria University, Ibrahimia, P.O. Box 426, Alexandria 21321, EGYPT

³ Department of Physics, Faculty of Science, Beirut Arab University, Lebanon

*E-mail: ashrafmoustafa@yahoo.com

Received: 1 March 2020 / Accepted: 15 April 2020 / Published: 10 June 2020

Mineral calcareous deposits are a current challenge in industrial water systems. The antiscalant properties of *Prunus dulcis* (Almond) leaf extract were tested using different chemical and electrochemical techniques. Fourier transform infrared spectroscopy (FTIR) was used to identify the functional groups of almond leaf extract. Static anti-scaling, conductivity, chronoamperometry, as well as optical photographic studies showed that almond leaf extract acts as a safe, ecofriendly antiscalant for steel in brine solution. Electrochemical impedance spectroscopy (EIS) technique and Potentiodynamic polarization curves measurements were used to test the inhibitive effect of Almond leaf extract on the corrosion of mild steel in brine solution. The results obtained showed that almond leaf extract acts as mixed type inhibitor. The corrosion inhibition increases by increasing the concentration of the extract up to a critical concentration. It is recommended to use 400 ppm of almond leaf extract to impede the formation of scale deposits and provide an acceptable level of corrosion inhibition.

Keywords: Green Anti-Scalant, Almond Leaf, mild steel, Corrosion Inhibition, scale Deposition

1. INTRODUCTION

Scale deposition is a conflict that arises with water that contains soluble salt minerals. Economic losses and the harmful effects of deposition of the scale can be found in several forms: loss of production capacity due to routine and unexpected shutdowns to remove the scale; increased pumping expenses and reduced heat transfer in heating systems [1]. Local corrosion in the cooling water system is another problem that accompanies deposited scales because of the formation of a small anode area under the calcification layer with respect to a large cathode. This situation is actually caused by lower of oxygen concentration underneath the deposit layer [2]. Deposition of scale deposition is regulated primarily by

the use of antiscalants. For cooling water systems and desalination processes, several polymer scale inhibitors are used for scale control. However, the environmental issues and discharge constraints have changed the chemistry of scale-inhibitors to low-cost biodegradable green antiscalants [1]. Different plant extracts have been evaluated for inhibition of CaCO_3 deposition [3-7]. Such extracts are a rich source of naturally synthesized chemical compounds which can be extracted using procedures that are low-cost. Various natural products have been used in different applications as corrosion inhibitors [8-14]. Several plant extracts have been recorded as corrosion inhibitors for steel in simulated seawater solution [15-25]. Abdel-Gaber *et al.* examined the efficiency of the olive leaf extract (*Olea europaea* L) as scale and corrosion inhibitor for mild steel in brine solution [5]. The data showed that addition of the extracts even at a low concentration (5 ppm) hinders the surface coverage of the electrode surface by deposits, indicating that it can be used as a good antiscaling agent. In addition, it offers reasonable efficiency as corrosion inhibitor for steel in brine solution. Our previous studies have tested the role of different plant extracts in inhibiting the formation of scales. This can be accomplished by chelating calcium ions with molecules extracted from the plant that prevent the formation of calcium carbonate or by suppressing the deposition of calcium carbonate by adsorption of these molecules over the metal surface [3-7, 17, 26].

The innovation of this work is to test a new plant extract to reduce the formation of scales and to serve as corrosion inhibitor of steel in brine solution. In addition, an appropriate concentration of the extract to act as anti-scaling and as an inhibitor for corrosion of steel in the brine solution will be derived.

2. EXPERIMENTAL STUDIES

2.1. Solution Preparation and extract procedure

Distilled water and analytical reagent-grade Ethylenediaminetetraacetic acid (EDTA), NaCl, NaHCO_3 , Na_2SO_4 and CaCl_2 purchased from Sigma-Aldrich Company were used for preparing solutions. CaCl_2 brine solution and Almond stock solutions were prepared as reported previously [8, 25].

2.2. FTIR analysis

FTIR analysis of the plant extract was carried by FTIR 8400S Shimadzu in the spectral region between 4000 and 500 cm^{-1} .

2.3. Static anti-scaling, Conductivity experiments and Electrochemical Studies

Screening examinations, static inhibition experiments and conductivity studies have been performed as described previously to evaluate anti-scaling behavior [26-28].

Chronoamperometry, Electrochemical impedance (EIS) and potentiodynamic polarization curves measurements were done using ACM instruments (UK). The detailed description of electrodes and pre-experimental procedures used during this investigation was reported in a previous study [26, 29].

2.4 Optical study

Optical Photographs were taken with a 12-megapixel canon camera that is attached to a personal laptop.

3. RESULTS AND DISCUSSION

3.1. FTIR Analysis

The Almond IR spectrum, figure 1, shows absorption bands for several functional groups including C=O, C-O O-H, C=C as well as C-H stretching bands. It has been reported that [30, 31] almond leaf extract contains a variety of organic compounds including glycosides and anthraquinone where the latter (Figure 2) is considered to be a major constituent. The predicted spectrum bands of the hydrolyzed form of anthraquinone are in a good agreement with those obtained from the measurement of FTIR spectroscopy.

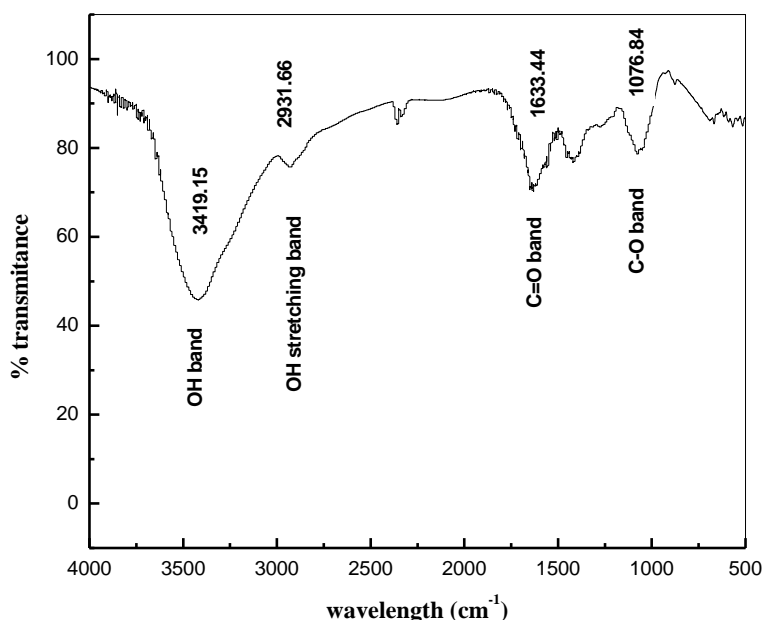


Figure 1. FTIR spectra of Almond plant leaf extract.

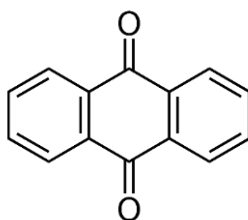


Figure 2. Anthraquinone

3.2. Antiscalant behavior of Almond leaf extract

3.2.1. Static Anti Scaling Data

Anti-scaling efficiency was investigated using the calcium carbonate deposition method [26,27]. The concept was to heat brine solution with and without the scale inhibitor for 10 hours at temperature of 80 °C. The concentration of calcium ion was then determined by titration with EDTA. Anti-scaling efficiency was calculated using the relation:

$$\text{Anti-scaling efficiency} = [(C_1 - C_0)/(C_2 - C_0)] \times 100$$

where C_0 and C_1 are the calcium ions concentrations without and with scale inhibitor, while C_2 was calcium ions concentration prior to the experiment.

Figure 3 shows the anti-scaling efficiency of almond leaf extract obtained from static measurements, indicating that the efficiency increases with an increase in the concentration of the extract up to 400 ppm after which a slight increase is achieved. This suggests that the leaf extract could be used as efficient antiscalant for CaCO_3 deposits.

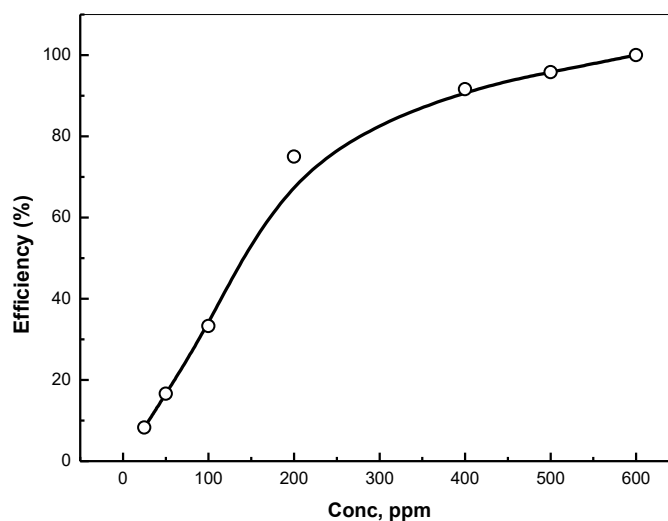


Figure 3. Variation of the anti-scaling efficiency with the concentrations of Almond leaf extract.

3.2.2. Conductivity Measurements

Figure 4 shows that the conductivity of the solution tends to increase linearly by increasing the added volume of Na_2CO_3 up to the point where the solution is supersaturated, and rapid precipitation of CaCO_3 begins with a sharp decrease in conductivity. After complete precipitation, the addition of extra Na_2CO_3 produces more ions in the solution, which again increases the conductivity. The increase in the concentration of almond leaf extract leads to an increase in the amount of Na_2CO_3 required for deposition of CaCO_3 to higher values.

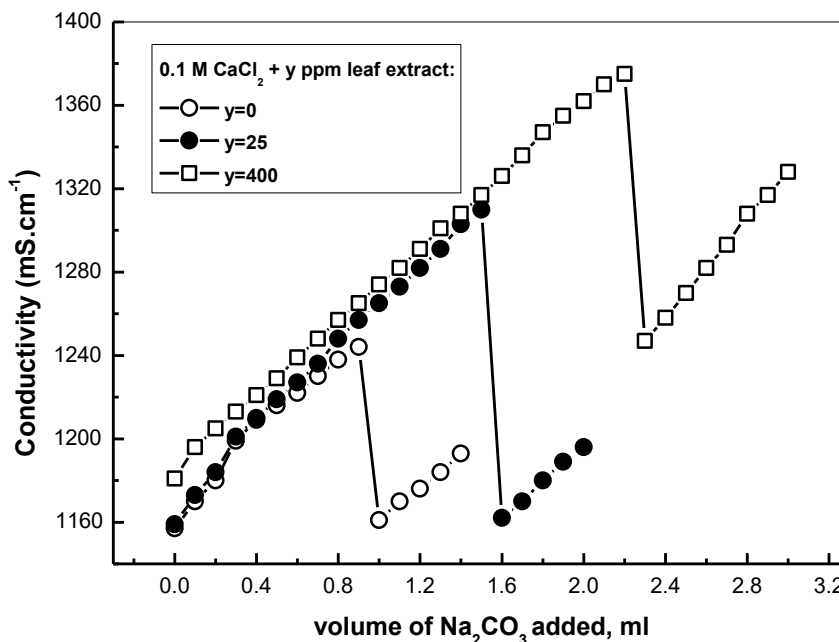


Figure 4. Variation of solution conductivity of CaCl₂ with the amount of Na₂CO₃ added in the absence and presence of different Almond leaf extract concentrations.

Figure 5 shows that the supersaturation volume increases with the increase in the concentration of leaf extract indicating that it is capable of hindering the supersaturation due to the adsorption of the extracted molecules on the active sites of the growing crystals, which leads to the liquefaction of suspended solids and thus reduces the rate of crystal growth [3, 26]. This confirms the results of the static anti-scaling data.

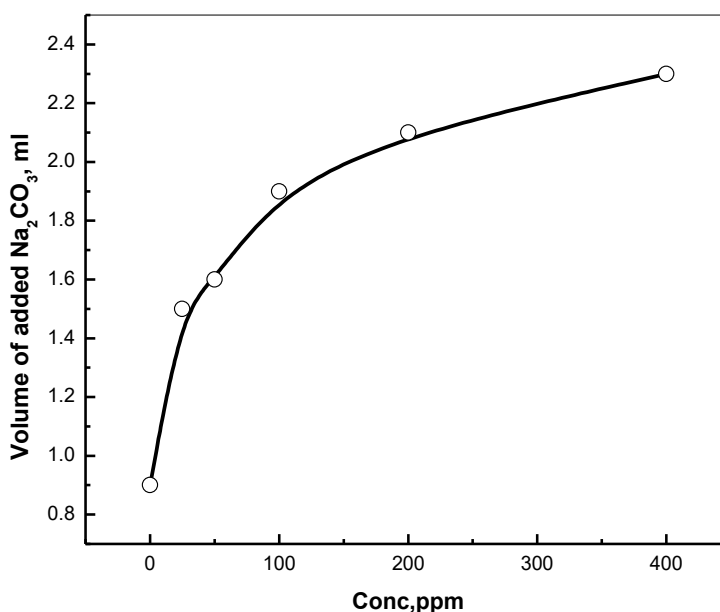


Figure 5. Variation of supersaturation volume of Na₂CO₃ as function of Almond leaf extract concentration.

3.2.3. Chronoamperometry Measurements

The current density-time curves shown in Figure 6 suggest that the current density was significantly reduced before reaching a steady state value. This linear decrease of current is a result of the deposition of CaCO_3 scales over the steel surface [3]. Increased scale deposition shield the active surface area available for the electrochemical reactions and consequently reduce the current density values [3, 26]. The inset of figure 6 shows a zoomed view of the steady state current density variations. Non-zero steady state current density values indicate that the scale is porous and does not fully cover the metal surface. Figure 7 shows that a high current density is obtained in the absence of almond leaf extract which reveals a porous scale surface coverage. With an increase in the concentration of the leaf extract up to 400 ppm, the current density decreases due to the adsorption of the extracted molecules which cover the voids of the porous scale [26, 32]. The increase of the leaf extract, up to 600 ppm, slightly increases the current density to $0.06225 \text{ mA}\cdot\text{cm}^{-2}$. This can be due to substitution of scale deposits by almond leaf extract molecules which interferes with the process of crystal growth and formation [26, 33].

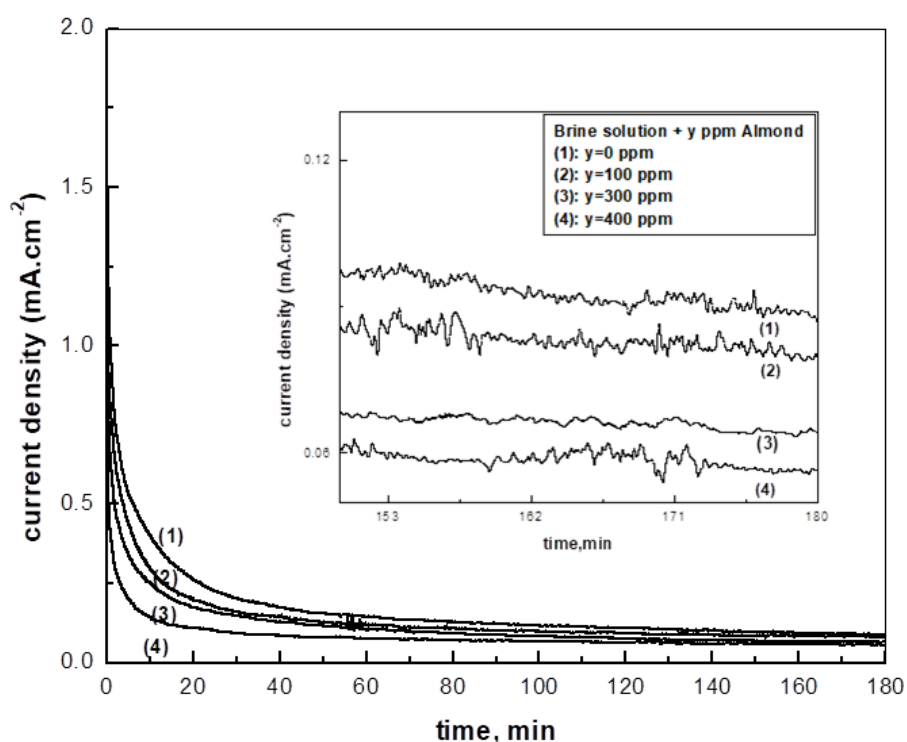


Figure 6. Chronoamperometry curves for polarized mild steel electrode in the CaCl_2 brine solution in the absence and presence of different Almond leaf extract.

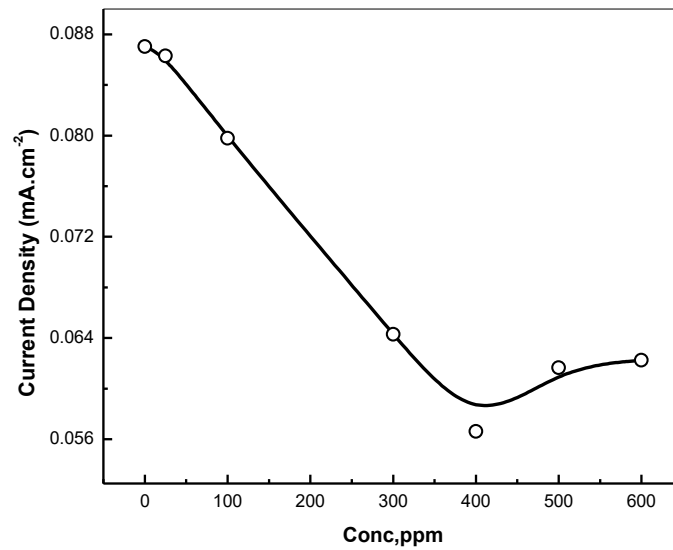


Figure 7. Variation of the current density obtained from the analysis of chronoamperometry curves at 180 min for polarized mild steel as function of Almond leaf extract concentration.

3.2.4. Optical Micrographic photos

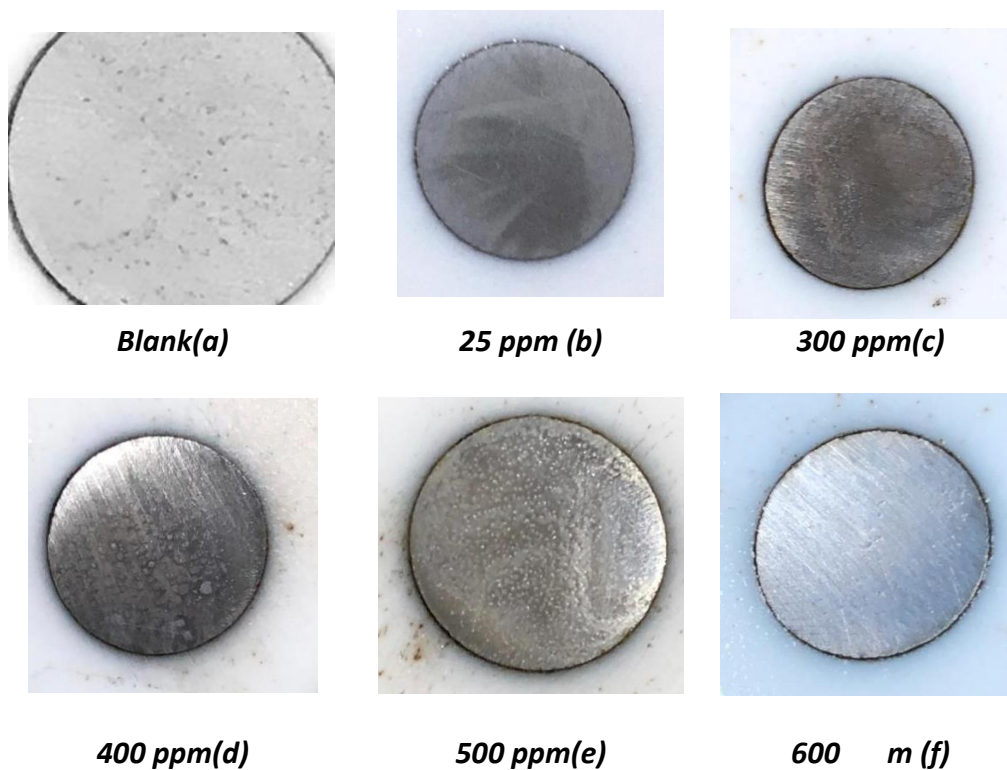


Figure 8 (a-f). optical micrographic photos of mild steel samples in CaCl₂ brine solution in the absence and presence of different Almond leaf extract concentrations

Figure 8 (a-f) shows the optical micrographic photos of mild steel samples in CaCl₂ brine solution in the absence and presence of different almond leaf extract concentrations. As seen, a complete surface

coverage by extremely dense scale crystals is observed in the absence of almond leaf extract, figure 8(a). Scaling deposits decrease with increasing extract concentrations where a smooth film of extracted molecules is formed over the mild steel surface.

3.3. Corrosion inhibitive action of almond leaf extract

3.3.1. Potentiodynamic polarization measurements

Figure 9 shows the potentiodynamic polarization curves for mild steel in brine solution in the absence and presence of different concentrations of almond leaf extract. The addition of almond leaf extract shifts the corrosion potential to more negative values. Since the greatest shift in the corrosion potential of almond leaf extract is about 40 mV, which is less than 85 mV, almond leaf extract can be considered as a mixed-type inhibitor for mild steel corrosion in brine solutions [34]. It is worth to mention that increasing the extract's concentration to 400 ppm not only suppresses the anodic dissolution of mild steel but also accelerates the oxygen reduction process at the cathodic sites leading to a higher current density values compared to 200 ppm.

The limiting current shown in the anodic part of the polarization curve in the presence of the leaf extract indicates that the diffusion of the corrosive species to the metal surface is impeded.

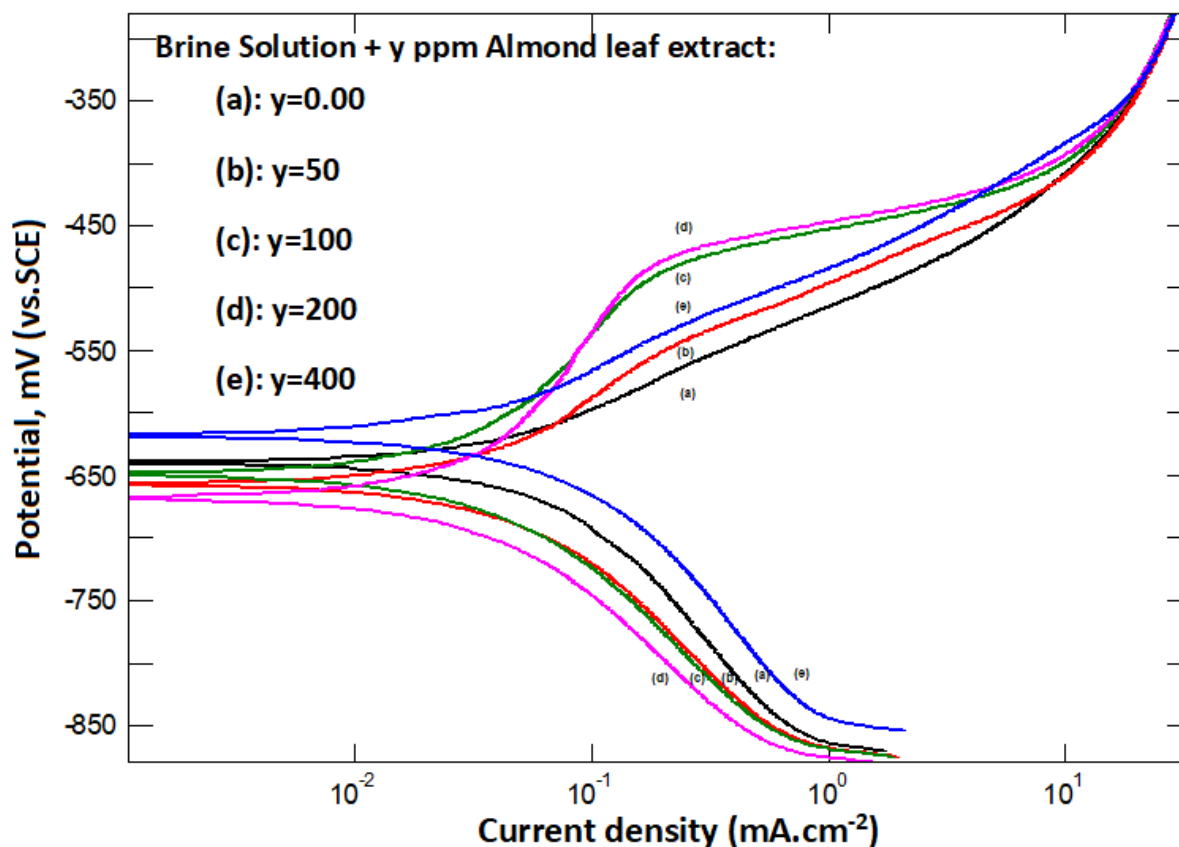


Figure 9. potentiodynamic polarization curves for mild steel in brine solution in the absence and presence of different concentrations of almond leaf extract.

The electrochemical polarization parameters together with inhibition efficiency (η) were given in Table 1. The inhibition efficiency (η) was calculated using the relation:

$$\eta = [(i_0 - i)/i_0] \times 100$$

Where i_0 and i , are the corrosion current densities in the absence and the presence of almond leaf extract, respectively.

The tabulated data showed that the corrosion current density (i) decreases with an increase in the concentration of almond leaf extract up to 200 ppm where the inhibition efficiency is 38.2. It is observed that at 400 ppm of the leaf extract, η decreased to 17.6. This drop can be attributed to the antagonistic effect of the ingredients extracted from the almond leaf above 200 ppm. Even so, the corrosion of steel in brine solution is still inhibited. The change in the anodic Tafel slope β_a can be explained by the modification of anodic dissolution process due to the adsorption of the extracted molecules at the active sites [35]

3.3.2. Electrochemical Impedance Spectroscopy

Figure 10 shows a good fit of the experimental results, plotted in Bode format, of mild steel in brine solution containing 200 ppm almond leaf extract with the equivalent circuit model (inserted in figure 10). The equivalent circuit used, includes the resistance elements R_s , R_2 , and R_{ct} and the constant phase elements CPE_1 , CPE_2 in addition to the Warburg diffusion W . The charge transfer resistance (R_{ct}), is a measure of electron transfer across the surface and is inversely proportional to corrosion rate.

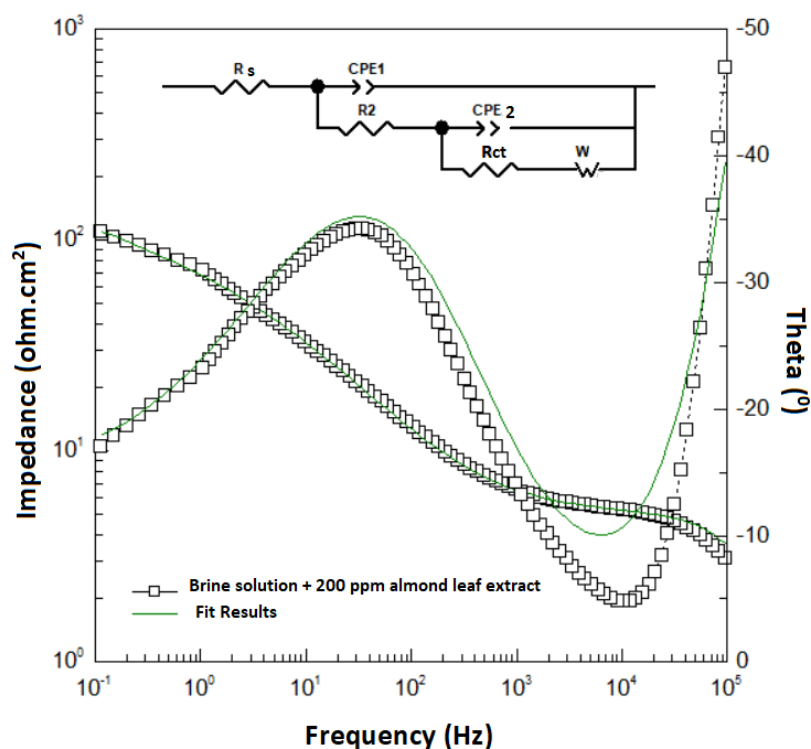


Figure 10. The experimental and computer fit results of the Bode impedance and Bode theta plots with the corresponding equivalent circuit model of mild steel in brine solution containing 200 ppm almond leaf extract

Figure 11 shows the Bode impedance plots for mild steel in brine solutions in the absence and presence of different concentrations of almond leaf extract. The values of the modulus impedance obtained at minimum frequency (R_{min}) have been reported to show the same trend as that of the charge transfer resistance (R_{ct}) [36-38]. For simplicity, the value of R_{min} is used in this study as a measure of corrosion resistance. The increase in the concentration of almond leaf extract up to 200 ppm increases the R_{min} values, as shown in Table 1. Any further increase in the concentration of the leaf extract therefore reduces the R_{min} values. This may be due to the antagonistic effect of the chemical ingredient extracted from the leaf of almonds at a certain concentration [12, 39]. The impedance measurements data are consistent with data obtained from polarization measurements.

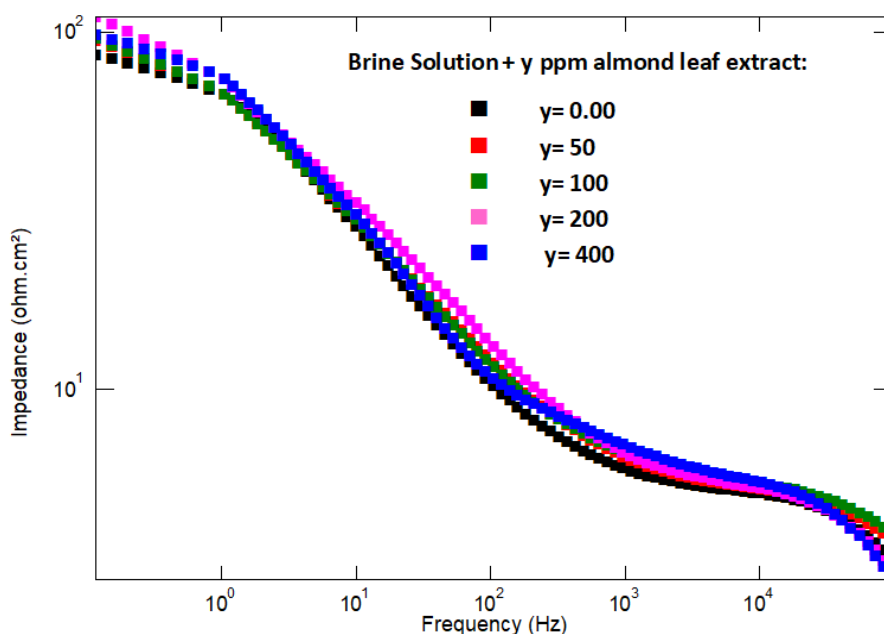


Figure 11. Bode impedance spectra of mild steel brine solutions in the absence and presence of different almond leaf extract concentrations

Table 1. The electrochemical polarization and impedance parameters for the corrosion of mild steel in brine solutions containing different concentrations of almond leaf extract respectively at 30 °C.

| Conc. (ppm) | $-E_{corr}$ (mV vs. SCE) | β_a | β_c | i (mA cm ⁻²) | η | R_{min} (ohm.cm ²) |
|----------------|-----------------------------|-----------|-----------|--------------------------------|--------|-------------------------------------|
| | | mV/decade | | | | |
| Blank | 624 | 86 | 203 | 0.0526 | - | 82 |
| 50 | 638 | 116 | 181 | 0.0370 | 29.6 | 90 |
| 100 | 635 | 201 | 180 | 0.0334 | 36.5 | 91 |
| 200 | 668 | 267 | 160 | 0.0325 | 38.2 | 106 |
| 400 | 602 | 115 | 170 | 0.0433 | 17.6 | 95 |

Based on the results obtained from anti-scaling measurements, it could be concluded that 400 ppm of almond leaf extract functions effectively as an antiscalant. On the other hand, adding 400 ppm to the brine solutions has an inhibition efficiency of 17.6 for the corrosion of mild steel. It is therefore recommended that 400 ppm of almond leaf extract be used to prevent scale deposition with an acceptable degree of inhibition.

4. CONCLUSIONS

- Almond leaf extract acts as an effective antiscalant with an acceptable level of corrosion inhibition.
- It is recommended to use 400 ppm of almond leaf extract to inhibit the formation of scale deposits with an adequate level of corrosion inhibition.

References

1. D. Hasson, H. Shemer, A. Sher, *Ind. Eng. Chem. Res.*, 50 (2011) 7601.
2. R. Sabzi, R. Arefinia, *Corros. Sci.*, 153 (2019) 292.
3. A. M. Abdel-Gaber, B.A. Abd-El-Nabey, E. Khamis, D.E. Abd-El-Khalek, *Desalination*, 230 (2008) 314.
4. A. M. Abdel-Gaber, B.A. Abd-El-Nabey, E. Khamis, H. Abd-El-Rhmann, H. Aglan, A. Ludwick, *Int. J. Electrochem. Sci.*, 7 (2012)11930.
5. A.M. Abdel-Gaber, B.A. Abd-El-Nabey, E. Khamis, D.E. Abd-El-Khalek, *Desalination*, 278 (2011) 337.
6. E. Khamis , E. El-Rafey, A.M. Abdel-Gaber, A. El-Hefnawy, M.S. El-Din. *IOP Conference Series: Mater. Sci. Eng.*, 301 (2018) 012149.
7. E. Khamis, E. El-Rafey, A.M. Abdel-Gaber, A. El-Hefnawy, N. Galal El-Din Shams El-Din, M. Salah El-Din Esmail Ahmed, *Desalin. Water. Treat.*, 57 (2016) 23571.
8. R.S. Al-Moghrabi, A.M. Abdel-Gaber and H.T. Rahal., *Int. J. Ind. Chem.*, 9 (2018) 255.
9. R.S. Al-Moghrabi, A.M. Abdel-Gaber and H.T. Rahal, *Prot. Met. Phys. Chem.*, 5 (2019) 603.
10. K.M. Hijazi, A.M. Abdel-Gaber, G.O.Younes , *Int. J. Electrochem. Sci.*, 10 (2015) 4366.
11. K. M. Hijazi, A.M. Abdel-Gaber, G.O.Younes, *Int. J. Electrochem. Sci.*, 10 (2015) 4779.
12. M. Lebrini, F. Robert, A. Lecante, C. Roos, *Corros. Sci.*, 53 (2011) 687.
13. A.M.Abdel-Gaber, E. Khamis, H. Abo-El Dahab, S. Adeel. *Mater. Chem. Phys.*, 109 (2008) 297.
14. A.M. Abdel-Gaber, H.T. Rahal, F.T. Beqai, *Int. J. Ind. Chem.*, 9 (2020) 1.
<https://doi.org/10.1007/s40090-020-00207-z>
15. E. Akbarzadeh, M.M. Ibrahim, A.A. Rahim, *Int. J. Electrochem. Sci.*, 6 (2011) 5396.
16. A.M. Abdel-Gaber, B.A. Abdel-Nabey, M. Saadawy, *Mater. Corros.*, 63 (2012) 161.
17. D.E. Abd-El-Khalek, A.M. Abdel-Gaber, *Port. Electrochim. Acta*, 30 (2012) 247.
18. A. Pradityana, A. Shahab, L. Noerochim, D. Susanti, *Int. J. Corros.*, 2016 (2016).
<https://doi.org/10.1155/2016/6058286>
19. H. Challouf, N. Souissi, M.B. Messaouda, R. Abidi, A. Madani, *J. Environ. Prot.*, 7 (2016) 532.
20. A. D.Arulraj, J. Prabha, R. Deepa, B. Neppolian, V.S. Vasantha , *Mater. Res. Express*, 6 (2018) 036527.
21. W.Ebdelly, S.B. Hassen, X.R. Nóvoa, Y.B. Amor, *Prot. Met. Phys. Chem.*, 55 (2019) 591.
22. K.Nasr, M. Fedel, K. Essalah, F. Deflorian, N. Souissi, *Anti-Corros. Method. M.*, 65 (2018) 292

23. N.K.Othman, S. Yahya, M.C. Ismail, *J. Ind. Eng. Chem.*, 70 (2019) 299.
24. E. Alibakhshi, M. Ramezanzadeh, S.A. Haddadi, G. Bahlakeh, B. Ramezanzadeh, M. Mahdavian, *J. clean. prod.*, 210 (2019) 660.
25. S.P. Palanisamy, G. Maheswaran, A.G. Selvarani, C. Kamal, G. Venkatesh, *J. Build. Eng.*, 19 (2018) 376.
26. R. H. Khaled, A. M. Abdel-Gaber, H.T. Rahal, R. Awad, *Desali. Water Treat.*, 180 (2020) 117.
27. J.C hen, H. Xu, J. Han, C. Wang, Q. Wu, C. Li, *Chem. Eng. Technol.*, 42 (2019) 444.
28. S. Zhang, H. Qu, Z. Yang, C. E. Fu, Z. Tian, W. Yang, *Desalination*, 419 (2017) 152.
29. H.T. Rahal, A.M. Abdel-Gaber, G.O. Younes, *Chem. Eng. Commun.*, 203 (2016) 435.
30. U. Tiwari, D. Nishi , S. Kaushik, *Int. J. Curr. Microbiol. Appl. Sci.*, 4 (2015) 728.
31. A.B. Muhammadu, A. Hassan, R.M. Okezi, *Niger. Chem. Res.*, 22 (2017) 31.
32. M.K. Shahid, Y.G. Choi, *J. Membr. Sci.*, 546 (2018) 61.
33. T. Chen, A. Neville, M. Yuan, *J. Petrol. Sci. Eng.*, 46 (2005) 185.
34. A. Boutouil, I. Elazhary, M.R. Laamari, H. Ben El Ayouchia, H. Anane, M.El Haddad, *J. Adhes. Sci. Technol.*, 34 (2019) 1.
35. A. Singh, I. Ahamad, M.A. Quraishi, *Arab. J. Chem.*, 9 (2016) S1584.
36. B. A. Abd-El-Nabey, S. El-Housseiny, E. Khamis, A.M. Abdel- Gaber, *Chem. Ind. Chem. Eng. Q.*, 23 (2017) 169.
37. H.T. Rahal, A.M. Abdel-Gaber, R. Awad, B.A. Abdel-Naby. *Anti-Corros. Method. M.*, 65 (2018) 430.
38. H.T. Rahal, A.M. Abdel-Gaber, R. Awad, *Chem. Eng. Commun.*, 204 (2017) 348.
39. A.M. Abdel-Gaber, B.A. Abd-El-Nabey, I.M. Sidahmed, A.M. El-Zayady, M. Saadawy, *Corros. Sci.*, 48 (2006) 2765

© 2020 The Authors. Published by ESG (www.electrochemsci.org). This article is an open access article distributed under the terms and conditions of the Creative Commons Attribution license (<http://creativecommons.org/licenses/by/4.0/>).